Heliyon 9 (2023) e21860

Contents lists available at ScienceDirect

Heliyon

journal homepage: www.cell.com/heliyon

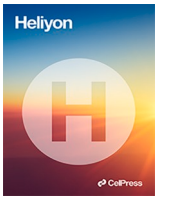

Ammonium concentration in stream sediments resulting from decades of discharge from a wastewater treatment plant

María Tijero Martín, Lucía Valdepeñas Polo, Javier González Yélamos, Jaime Cuevas Rodríguez *

Department of Geology and Geochemistry, Universidad Autónoma de Madrid, 28049, Madrid, Spain

ARTICLE INFO

Keywords:
ammonium
Geo-indicator
WWTP
wastewater
clay sediment

ABSTRACT

A study of ammonium pollution in the sediments of a stream that receives wastewater treatment plant (WWTP) discharge has been carried out. It is urgently necessary to find environmental indicators that can help prevent and detect potential contamination of water, as water is an increasingly scarce resource. To understand the behaviour of ammonium ions introduced by a historical (50-year) contamination process, vertical boreholes were drilled in the stream banks to depths between 30 and 120 cm. Moisture, pH, ammonium (soluble and exchangeable), and clay fraction content were analysed. The variation profile of these parameters was evaluated as a function of depth to determine factors related to the distribution of ammonium in several locations along the stream banks.

The ammonium concentration was asymmetrically distributed among samples collected in near-surface locations, with ammonium concentrations between 0.3048 mmol/kg soil and 0.0007 mmol/kg soil. Ammonium was typically concentrated at sediment depths of 30–40 cm, which also exhibited the highest clay fraction content. High positive correlations were detected ($r > 0.8$; $p < 0.0001$) among the different ammonium variables (exchanged and dissolved species). No contamination effect was observed below 60–70 cm depth, which was due to ammonium retention in a natural barrier layer of clayey sediment.

The clays in our study area (previously identified as smectite, a 2:1 sheet silicate) were able to control the contamination by retaining ammonium in the interlayers, which retarded nitrification. It is suggested that clay could serve as a geo-indicator of ammonium pollution evolution.

1. Introduction

Difficulties in water quality preservation and remediation of persistent soil pollution constitute the main threats to future ecosystem biodiversity, safe water resource availability and general human health [1]. One out of 8 deaths are caused by pollution in the EU (European Union), and most of these deaths are due to cancer diseases attributed to increased environmental degradation. Thus, there is an urgent need to control and prevent environmental burdens associated with pollution sources to achieve the goal of zero pollution [2]. Nearly 80 % of the world's population is exposed to high water hazard levels, which are partially mitigated in rich countries by investments in the treatment of used water or in safe soil and water protection systems [3]. The scarcity of water with the potential for human use will be further compromised by climate change. More intense and frequent summer droughts in semiarid

* Corresponding author.
E-mail address: jaime.cuevas@uam.es (J. Cuevas Rodríguez).

https://doi.org/10.1016/j.heliyon.2023.e21860
Received 12 May 2023; Received in revised form 27 October 2023; Accepted 30 October 2023
Available online 31 October 2023

regions and presumably humid regions will hinder water quality by altering the concentrations of nutrients derived from urban or agricultural discharges [4,5]. Among these nutrients, nitrogen is one of the most important threats to water resources [6].

The soil concentration of nitrogen compounds is caused both by anthropogenic sources and natural biogeochemical processes [7], with anthropogenic sources having the greatest impact on the environment. Nitrogen pollution derives, for instance, from landfill leachate runoff, the deposition of waste from the agricultural sector on soil, or industrial and municipal discharges that are not appropriately treated [8,9].

The effects of nitrogen on the environment include increased water acidity, eutrophication, and toxicity due to high concentrations in both surface water and groundwater, which limits the use of such waters for human consumption, as toxic levels of nitrogen are detrimental to public health and put the survival of organisms at risk [10].

Wastewater treatment plants (WWTPs) are designed to reduce nitrogen, phosphorus and dissolved organic carbon (DOC), among other purposes. The historically low efficiency of these processes means that discharges to river systems contain a nutrient load that alters the global nitrogen cycle [11]. In WWTPs, nitrogen compounds exist mainly as ammonium derived from two sources: (1) the influent wastewater and, if the activated sludge biological reactor is not efficient (i.e., it has anaerobic conditions), (2) the anaerobic digestion liquid after treatment [12]. Old facilities that have not been updated are a significant source of nitrogen loading to river systems [13]. WWTPs are designed to work for decades, and it is practically impossible to predict their performance in response to catchment changes or the need for adaptations to fulfil legal requirements [14]. Conventional procedures implemented and improved during the second half of the 20th century focused on treating high loads of urban DOC by primary aeration and aerobic activated sludge tanks with the precipitation of excess phosphate in the decanted sewage sludge. They were later modified to include an anoxic stage to allow nitrification and denitrification cycling to remove nitrogen nutrients.

Ammonium is an inorganic pollutant with relatively high mobility [15]. This mobility depends on (1) adsorption due to cation exchange with clays, which depends on pH, temperature, humidity and nitrification processes, and (2) volatilization that may occur depending on climate and that is increased by the rise of temperature and pH [16]. Adsorption slows the mobility rate of contaminants relative to the average velocity of water flow [17]. In aqueous solutions with low and neutral pH values, cation exchange occurs in the interlaminar region of clay minerals phyllosilicates with a μm particle size [18–20]. At pH values above neutral, metal oxy-hydroxides may play an important role in ammonium adsorption due to the negative charges that develop on the edges of clay lamellar structures or on the surface of free oxy-hydroxides. Adsorption by metal oxy-hydroxides depends on the pH and the point of zero charge of the metal-oxygen terminations. In 2:1 clay minerals, ammonium fixation can become irreversible because ammonium is adsorbed in its dehydrated form between lamellae [21,22]. Cations with a low charge/hydrated radius ratio, such as NH_4^+ or K^+, tend to remain dehydrated in clay surfaces with a relatively large radius and are preferentially adsorbed [23]. This mechanism is presumed to favour ammonium retention in the smectites among the arkosic sediments in the current study area; in addition, the partition constants (Kd) of this type of clay and other similar clays are high [24,25].

Ammonium concentrations can be decreased naturally by nitrification processes driven by nitrifying microorganism activity. These processes occur under aerobic conditions and may proceed even in anoxic sediment environments with limited NO_2^- and NO_3^- production via MnO_2 reduction processes [26–29]. Nitrification is characteristically associated with high concentrations of DOC and inorganic dissolved ions (chloride, ammonium, ferrous iron, sodium, and potassium) in landfill leachate plumes [30,31]. Natural attenuation (NA) is observed to be effective at distances of hundreds to 1 km with relatively long interaction times, as NA is limited by

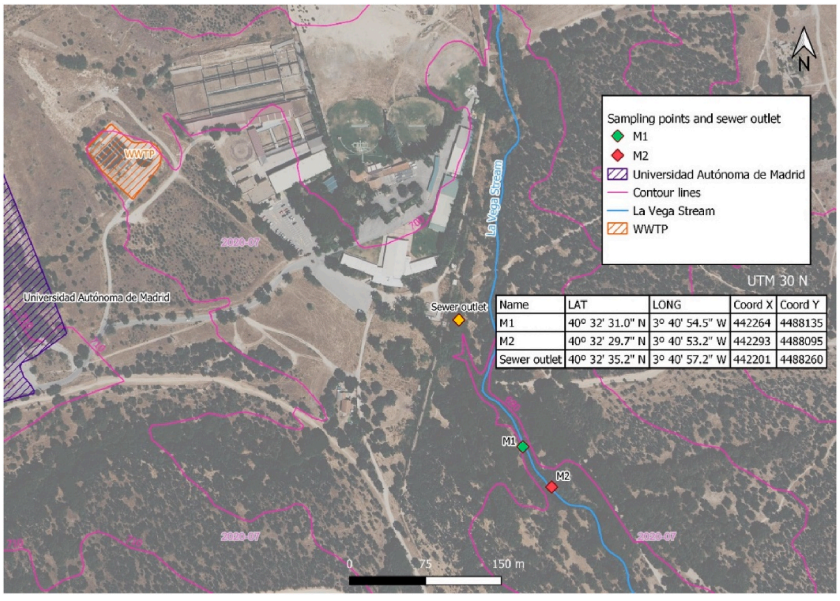

Fig. 1. Site location geographic coordinates and sampling points.

slow reaction times [32]. These authors remarked that these core processes are unlikely to contribute to the natural attenuation of NH_4^+ in the short term, although sorption of NH_4^+ is mainly controlled by ion exchange and leads to the retardation, but not the destruction, of contaminants. This retardation may increase the time available to perform or assess remedial measures, if required, and should be considered when determining whether NH_4^+ has been transformed or has reached its maximum pollution extent.

In this work, the distribution of ammonium contamination from a WWTP in the arkosic sediments of a stream channel was analysed in detail. Preliminary studies indicated an increasing concentration of ammonium with depth until 40–50 cm. Therefore, several samplings at greater depths were carried out to assess the depth of soil affected by the increase in concentration. On this basis, the origin and evolution of ammonium contamination are discussed considering that a significant improvement in WWTP performance was implemented in September 2019. The sediment data described in this work were acquired from November 2020 to May 2021. The objective of this study was to determine whether ammonium retention in clayey sediments is a reliable signature of a previously existing pollution source and to establish how this retention could be affected by natural attenuation mechanisms. The assessment of the use of clay minerals as geo-indicators of ammonium contamination will open new opportunities for natural controls to monitor and prevent pollution from urban wastewaters.

2. Environmental setting

2.1. Site location

The area of study is located in “Monte Valdelatas”, declared a preserved area of the Community of Madrid (Spain) in 1995 [33]. The stream under study (Fig. 1) belongs to the Tajo Hydrographic Basin [34], corresponding to the Tertiary detrital aquifer of “Madrid Manzanares - Jarama" [35]. Detritic materials are typical of the Madrid Tertiary Basin and include sands, silts and clays [36]. The texture is clayey, so permeability is very low at times, which causes hydromorphic soil characteristics [37].

2.2. WWTP characteristics

The Universidad Autónoma de Madrid (UAM) WWTP has been in operation since 1970. The system originally consisted of primary and secondary treatment stages with anoxic treatment and biological activated sludge aerobic treatment, followed by sludge settling in a rectangular continuous flow sedimentation tank of 3 m depth. The WWTP underwent significant remodelling in 2018 [38], which extended the activated sludge treatment capacity after the anoxic stage by incorporating the previous settling tank into the activated sludge stage and adding a new circular sedimentation tank as a clarifier. This allowed more efficient biological sludge separation and recirculation, with the aim of modifying the parameters of the effluent discharged to the nearby stream to meet the specifications of Spanish legislation on the treatment of urban wastewater [39]. This WWTP treats wastewater from the entire university campus along with stormwater (931 m^3 per day) [40].

Taking the above into account, it is quite likely that the UAM WWTP may have discharged effluent to the stream in excess of the limit of 10–15 mg/L total nitrogen permitted by Spanish legislation on the treatment of urban wastewater [39] for more than three decades. The major component of the total nitrogen was the ammonium cation. The output pH was approximately 7.0, and at this pH, the ammonium cation is stable in relation to ammonia gas, which constitutes more than 60 % of the ammoniacal nitrogen at pH 8.5 and above [41].

3. Sediment sampling

Sediments were sampled with a one-piece 5 cm diameter Eijkelkamp™ riverside auger for hard, stiff soils mixed with fine gravel.

A sequential sampling strategy was followed to delimit and capture typical depth profiles for the analysis of sediment ammonium contents. Detailed information on the samples collected for the study is given in Table 1. An initial prospective sampling point (M1) was used to check if there were variations in ammonium in the sediments and to test if the contamination was related to depth. Samples were taken near the surface (<15 cm) because of the difficulty of going deeper due to the presence of pebbles. Therefore, an alternative location was used to measure a 50 cm depth profile (M2).

To sample a transversal cross section of the stream, an area with well-defined banks was selected. A series of two profiles located on

Table 1
Sampling point information.

Point	Type	Date	Depth	Number	Stream bank
M1	Soil	October 23, 2020	15 cm	3	Right
M2A	Soil	November 06, 2020	50 cm	4	Central
M2B	Soil	November 30, 2020	77 cm	11	Right
M2C	Soil	March 26, 2021	77 cm	10	Left
M2D	Soil	April 16, 2021	120 cm	14	Right
M2E	Soil	April 16, 2021	68 cm	9	Central
M2C	Water	April 16, 2021	Surface	2	Central
M2E	Water	April 16, 2021	30–40 cm	1	Left

Number = number of samples.

the right and central sides of the stream banks (M2A and M2B) were taken, as variations in the distribution of ammonium were observed. To check the previously mentioned dynamics, samples were collected at the greatest possible depth (>60 cm) allowed by the sedimentary material. Finally, a series of samples were collected from both banks and the middle of the stream channel (M2C, M2D and M2E) to capture a 2D distribution including the bottom area of the channel excavated by the stream (see Table 1 and Figs. 1 and 2). This profile was useful for better understanding ammonium cation mobility in relation to the fluvial dynamics associated with this type of short course river flow.

Water samples were taken at two points on along the horizontal profile (M2C and M2E) and inside one of the boreholes to analyse the drained infiltrated water and its ammonium content compared to that of the stream water.

4. Methods of analysis

For the electrical conductivity (EC), pH, humidity [42], dissolved ammonium (d-NH_4^+), exchangeable ammonium (e-NH_4^+) and total ammonium (t-NH_4^+) were analysed [43], along with the mass percentage of the clay fraction [44]. Concurrently, water-soluble cations were analysed by ion chromatography, specifically performed to assess the representativeness of the ammonium content in the samples [45].

4.1. Physicochemical properties

Sediment samples from various depths were analysed for EC and pH. Soil (10 ± 0.05 g) was wetted with 25 ml of distilled water and shaken for 30 min. After settling of the material, the EC and pH of the supernatant were measured.

To measure the humidity of the samples, 5 g ± 0.05 g of soil was weighed and placed in an oven at 105 °C for 3 days.

4.2. Ammonium determination

A Thermo Fisher Scientific ammonium selective electrode was used for dissolved (d-NH_4^+) and total ammonium (t-NH_4^+) measurements [46]. For both measurements, 10 ± 0.05 g of soil was weighed. For d-NH_4^+ and t-NH_4^+ measurement, 25 ml of distilled water and 25 ml of KCl, respectively, were added to the soil. The supernatant (20 ml) was transferred to a 50 ml volumetric flask for later measurement with the selective electrode. Exchangeable ammonium (e-NH_4^+) was obtained by subtracting the dissolved ammonium from the total ammonium.

4.3. Clay mass percentage

As there is evidence that smectite or illite minerals (included, for instance, in bentonites and clayey sediments) could retain ammonium contamination by ion exchange [47], the percentage of clay present in the sediments was determined in the M2C-D-E transect.

The clay percentage was determined using a sedimentation method. A mixture of approximately 45 ± 0.05 g of sediment and 80 ml of distilled water was shaken vigorously and settled for 12 h. The sediment was shaken again and left to stand for 4 h, and then the first 5 ml of the suspended sediment was extracted (with an automatic pipette). This represents the depth at which particles smaller than 2

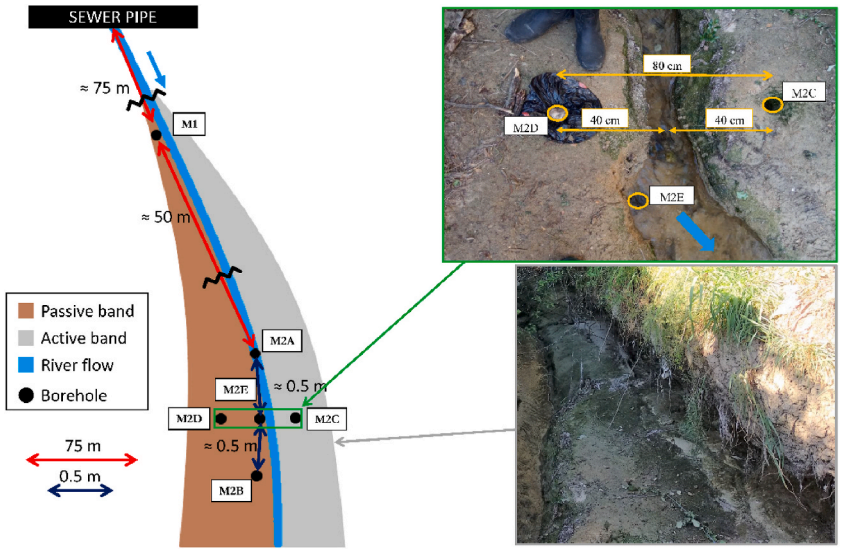

Fig. 2. Distribution sketch of boreholes in the study area. Images on the right side of the figure show real photos of the Section M2D-M2E-M2C.

μm do not settle according to Stokes' law (at 20 °C).

The clay obtained after drying the 5 ml suspension was weighed, and the value was extrapolated to the volume of water added. Clay weight is expressed as a percentage with respect to the dry weight of soil; the moisture content of each of the samples was previously evaluated.

4.4. Water-soluble cations

The samples were diluted 1:2 to avoid exceeding an EC of 500 μS/cm. Most cations were analysed by ion chromatography [48] using a Metrohm 802 compact IC with a conductivity detector (IC-CD). Additionally, electrical conductivity (EC), pH and alkalinity were determined by potentiometry on a Metrohm 888™ automatic instrument.

4.5. Statistical analysis

Descriptive statistics were calculated to assess how ammonium behaves in association with other variables in the analysed sediments. The mean, median and Pearson correlation coefficient were calculated, and the normality test (Shapiro–Wilk test with a significance level of 0.05) was performed to assess the distribution of all the parameters measured in the samples using OriginPro® 2023.

Q–Q plots were made with the Bernard score method at a 95 % level of confidence to test if the distribution of the parameters followed a lognormal distribution. Additionally, the nonparametric Kolmogorov–Smirnov test was applied to confirm the lognormal distribution.

5. Results

5.1. Descriptive statistics

An overview of the descriptive statistics for the measured variables in the studied stream and sediments is shown in Table 2.

Regarding the distribution, the Shapiro–Wilk normality test, with a significance level of 0.05, rejected normality for most parameters with a p value < 0.0001 (except for d-NH_4^+, p value 0.0111). The data obtained for dissolved, exchangeable and total ammonium were then log-transformed and presented in a Q–Q plot, which confirmed the lognormal distribution of the variables. The plotted data corresponding to the different forms of ammonium in the samples show at least two populations of data with linear trends in the Q–Q plot. The linear trend with the small number of samples indicates high ammonium concentrations that deviate from typical WWTP contamination levels (Fig. 3). These data were above the lognormal estimate and corresponded to the M2D profile for both d-NH_4^+ (7–28 cm depth) and e-NH_4^+ (7–41 cm depth).

The Kolmogorov–Smirnov nonparametric test was applied to d-NH_4^+, e-NH_4^+ and t-NH_4^+ to test their deviation (Table S1, supplementary material) from a lognormal distribution. Considering a decision level of 5 %, a lognormal distribution could not be rejected.

The Pearson coefficients indicated some significant correlations between variables (considering a significant correlation at $p < 0.01$; Table S2, Supplementary material). There were high positive correlation coefficients ($r > 0.8$; $p < 0.0001$) between the different ammonium variables (exchangeable and dissolved species), whereas variables such as EC and ammonium species concentration were negatively correlated with depth ($r < -0.51$; $p < 0.003$). pH and clay percentage showed significant correlations with other variables. pH increased with depth ($r = 0.44$; $p < 0.01$), and the clay percentage was related to e-NH_4^+ ($r = 0.45$; $p = <0.01$).

The statistical results, as will be described in the following sections, indicate a dependent relation between the different variables (pH, ammonium, etc.) and sample location. Other dependent factors, such as sediment dynamics (erosion and sedimentation processes), were qualitatively considered.

5.2. Ammonium distribution with depth at the sample points

The M1 data (Table S3; supplementary material) indicated variations in EC, pH, e-NH_4^+ and t-NH_4^+ from samples M1.10 to M1.15. The samples are identified in the text as M#.depth (cm). In only 5 cm, the pH changes from basic to slightly acidic. The ammonium at this point is mostly exchangeable and exhibits notable variation from samples M1.10 to M1.15, with values of 0.0901 mmol/kg soil to

Table 2
Descriptive statistics.

Parameter	Mean	Standard Dev.	Median	Max.	Min.	Range
Moisture (%)	14.3	3.48	13.3	25.8	11.3	14.5
EC (μS/cm)	64.5	40.9	58.4	248	11.3	273
pH	7.60	1.19	8.19	8.94	4.26	4.68
d-NH_4^+ (mmol/kg d.s.)	0.0092	0.0069	0.0081	0.0272	2.27E-4	0.0270
e-NH_4^+ (mmol/kg d.s.)	0.0540	0.0596	0.0392	0.3019	4.84E-4	0.3014
t-NH_4^+ (mmol/kg d.s.)	0.0625	0.0609	0.0470	0.3048	7.11E-4	0.3040

N = 51. d-NH_4^+: dissolved ammonium; e-NH_4^+: exchangeable ammonium; t-NH_4^+: total ammonium; EC: electrical conductivity. d.s.: dry soil.

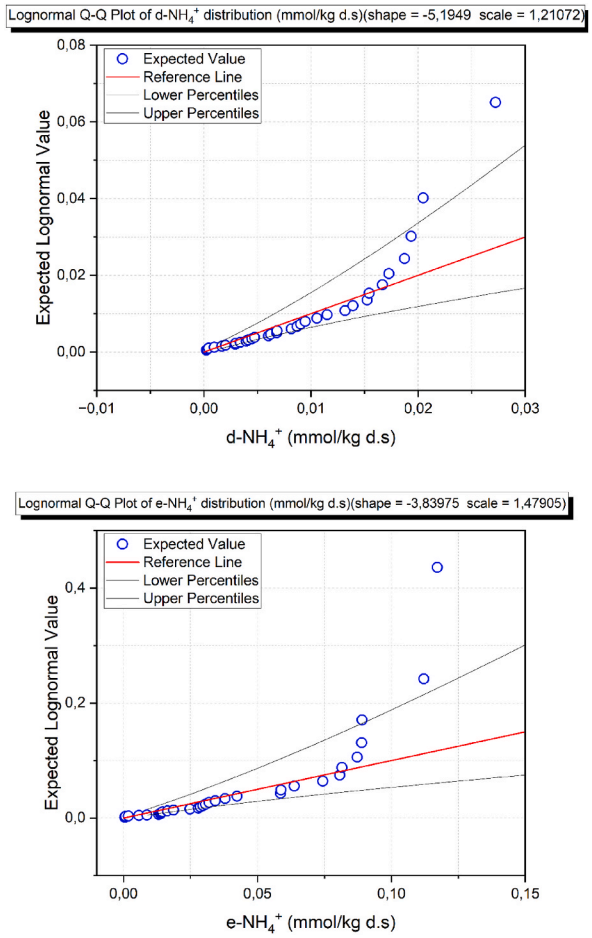

Fig. 3. Lognormal Q−Q plots showing the distribution of d-NH_4^+ and e-NH_4^+.

0.2915 mmol/kg soil, respectively. This group of samples represents shallow points with an increase in e-NH_4^+ with increasing depth, along with a decrease in pH, contrary to the trend indicated by the general statistical description.

Sampling point M2A was located within the stream channel to investigate a deeper section influenced directly by the stream water (Table S3, supplementary material; Fig. 2). The profile depth could be increased to check whether the variation trend persisted downstream of the first sampling point.

As the sampling point was in the centre of the channel, a higher percentage of moisture was measured in the shallowest sample (M2A.10). The distance between the surface of the bank and the bottom of the channel was approximately 30–35 cm. Sampling was initially performed on the excavated stream walls (30 cm) and continued through the bottom of the stream channel for another 20 cm. This emplacement (10 m long with well-defined banks) was used for several profile samplings in this work. Throughout the sampling process (6 months), a constant water level was observed every day (15 cm depth).

In all cases, the contribution of e-NH_4^+ to t-NH_4^+ was predominant. A variation in e-NH_4^+ was measured in samples M2A.25 and M2A.30, with values from 0.1377 mmol/kg soil to 0.0626 mmol/kg soil, respectively. Sample M2A.10, with a value of 0.3048 mmol/kg soil for t-NH_4^+, had the highest ammonium concentration among all the analysed sampling points at a pH of 8.5, at the limit of possible ammonia gas generation. Therefore, contamination was not strictly related to the proximity of WWTP discharge (approximately 100 m upstream), but presumably also related to the dynamics and particular characteristics of the sediments in the stream banks, such as clay content. In this case, for the borehole, the pH was generally more alkaline and homogeneous (7.3–8.5) than in the previous case, and the highest concentration was found near the surface. EC decreased, and pH returned to a slightly basic trend, whereas ammonium decreased sharply at 50 cm. The sample depth and proximity to the stream water (the sample was located 20 cm below the centre of the stream channel) seem to be factors influencing the location of the ammonium-concentrated (polluted) zone.

In the M2B profile, it was possible to drill a deeper borehole to 77 cm; this borehole was outside the stream channel to avoid the proximity of water (Table S3 in supplementary material). Within 25–40 cm, t-NH_4^+ was above the mean (0.0800–0.0600 mmol/kg), and in general, the pH was <8.0. The pH increased to 8.2–8.4 for the deeper samples (>70 cm) with the lowest ammonium contents, whereas near-surface samples (M2B.7 and M2B.15) presented slightly acidic values, and a trend towards neutral values was observed up to 25 cm.

EC showed decreasing values from the surface to M2B.25. Then, EC rose to 96 μS/cm at M2B.30, decreased to a minimum of 45 μS/cm at 48 cm, and remained relatively constant with increasing depth. Soil EC decreased with depth where a general drop in ammonium pollution was observed.

The M2A and M2B profiles provided information on different trends in ammonium concentration, pH and EC with regard to near-surface samples and ammonium pollution attenuation with depth. To confirm natural attenuation of ammonium at depth and to obtain more data on the evolution profiles from near-surface to deeper sediments, three new boreholes were drilled in a transect perpendicular to the stream water current (M2D, M2E and M2C) (Fig. 2) to allow comparisons with the banks and stream bed, including the quantification of the clay fraction.

The M2C profile (Table S4, supplementary material), located at the opposite bank from M2B (Fig. 2), showed very acidic pH values (close to the minimum, 4.3) from the surface to 25 cm (M2C.25), where the pH changed sharply to slightly basic (close to 8.0). The measured t-NH_4^+ concentration reached the peak in this profile at M2C.25 (0.1012 mmol/kg), followed by a gradual decrease with depth. EC had high values (up to 284 μS/cm compared to a global mean of 64 μS/cm) accompanying the lowest pH measured. EC decreased with increasing pH (basic conditions) at depths >30 cm.

At sampling point M2D (Table S5, supplementary material), it was possible to reach the greatest depth, 120 cm. Throughout the borehole, the pH values were between 7.0 and 8.0, with one exception (M2D.15; pH = 6.5). EC decreased gradually with depth without any significant changes on this bank with a similar location to M2B.

t-NH_4^+ decreased until sample M2D.20, from which it stabilized until 40 cm. From sample M2D.40, t-NH_4^+ gradually decreased again until reaching the minimum value among all the sampled points in sample M2D.120 with 0.0007 mmol/kg soil.

The maximum t-NH_4^+ in this section was measured in sample M2D.7 with a value of 0.1394 mmol/kg soil, which was second only to the value for sample M2A.10 (0.3048 mmol/kg soil) among all sampling points.

At sampling point M2E (Table S6, supplementary material), a sharp drop in conductivity from sample M2E.10 to M2E.18 was measured. From the acidic surface, the pH became increasingly basic until sample M2E.26, from which it remained stable until M2E.68. As in previous points, the predominant ammonium form was e-NH4+. t-NH4+ showed two peaks in samples M2E.26 and M2E.45.

A comparative analysis of the ammonium evolution of the M2C, M2D and M2E transects is shown in Fig. 4. The attenuation of ammonium pollution with depth was confirmed by these data. There was high variability between d-NH_4^+ and e-NH_4^+ in the near-surface samples (Fig. 5), whereas from 50 cm to greater depths, there was less dissolved ammonium than exchangeable ammonium.

A two-dimensional visualization of the changes in the analysed variables was built using Surfer® software (Surfer version 11.0.662. 2012. Golden software, Inc.).

The highest t-NH_4^+ concentrations (Fig. 6) were located at the margins of the stream, corresponding to sampling points M2D and M2C. In M2D, the contamination followed a uniform trend from the surface to approximately 50 cm depth, while in M2C, it was concentrated between 20 and 50 cm, with a decrease in concentration at the surface until 20 cm. With respect to the M2E sample, a relatively low ammonium concentration was found until 40 cm, where a band with a consistent ammonium concentration was maintained until 50 cm before a general decrease in concentration with depth occurred.

5.3. Clay mass percentage

The weight percentage of the clay fraction decreased notably in the first 40 cm of the M2E profile, coinciding with the zone of contact with the stream channel (Fig. 6). The M2D profile contained a band with a higher concentration of clay between 30 and 40 cm, and a similar trend was observed in the M2C profile from approximately 40-60 cm with slightly lower values. Fig. 6 shows an asymmetric band between 40 and 60 cm with higher clay contents that separated a shallower contaminated zone from another zone with very low ammonium concentrations at greater depths.

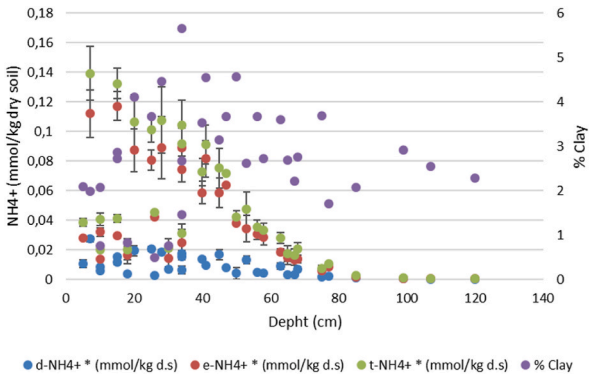

Fig. 4. Variations in clay percentage and ammonium concentration with depth in horizontal section M2D-M2E-M2C. d-NH_4^+: dissolved ammonium; e-NH_4^+: exchangeable ammonium; t-NH_4^+: total ammonium; EC: electrical conductivity. % Clay: Weight % of clay in the soil sample.

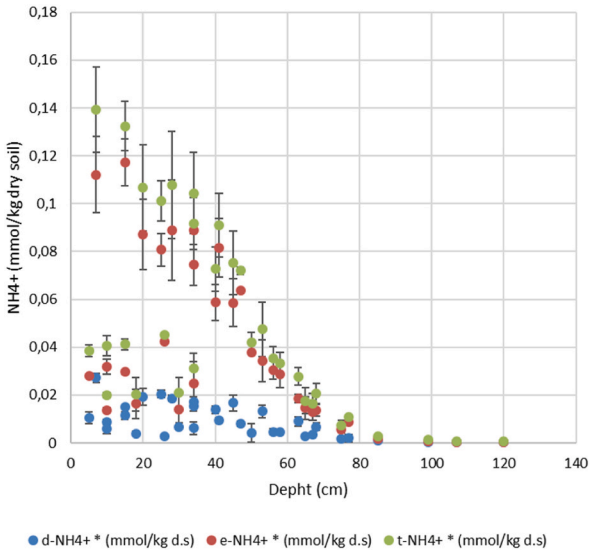

Fig. 5. Ammonium variation with depth in horizontal section M2D-M2E-M2C. d-NH_4^+: dissolved ammonium; e-NH_4^+: exchangeable ammonium; t-NH_4^+: total ammonium; CE: electrical conductivity.

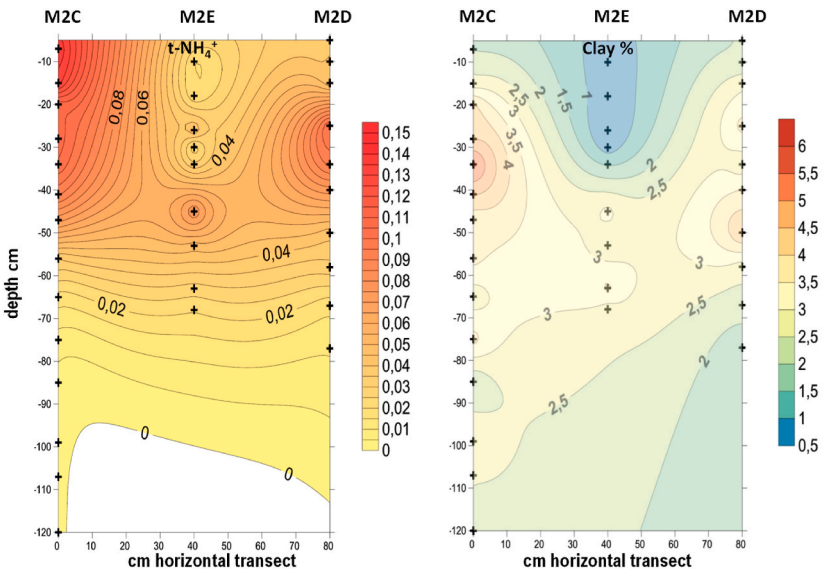

Fig. 6. 2D representation of t-NH_4^+ concentration as a function of depth in the M2C-E-D horizontal transect (left). Clay weight percentage in sediments as a function of depth (right). t-NH_4^+: total ammonium (mmol/kg dry soil).

Table 3
Results from sampling points M2C and M2E (water).

SAMPLE	M2C (drained borehole)	M2E (stream)
Na^+ (mg/L)	99.5 ± 0.8	117.6 ± 1.7
NH_4^+ (mg/L)	7.4 ± 0.2	0.5 ± 0.0
K^+ (mg/L)	12.9 ± 0.7	14.5 ± 0.6
Ca^{2+} (mg/L)	67.2 ± 0.9	21.1 ± 1.1
Mg^{2+} (mg/L)	6.2 ± 0.3	1.5 ± 0.5
pH	6.4 ± 0.1	6.9 ± 0.0
HCO_3^- (mg/L)	143.5 ± 0.2	27.8 ± 0.0
EC (μS/cm)	930 ± 13	640 ± 10

5.4. Water-soluble cations

Once the auger drilling of the M2C borehole was finished, stream water was collected (after the WWTP redesign) along with infiltrated water from the borehole bottom, pumped with the aid of a Tygon® tube attached to a polypropylene syringe. The analysed parameters are shown in Table 3.

The pH values of both water samples were slightly acidic. In sample M2C (water), the order of cations was $Na^+ > Ca^{2+} > K^+ > NH_4^+ > Mg^{2+}$. Ammonium had a content of 7.4 mg/L, and the lowest concentration corresponded to Mg^{2+}, with a value of 6.2 mg/L. This can be taken as additional evidence for the persistence of previous WWTP contamination, with a significant increase in dissolved bicarbonate that can be attributed to the oxidation of dissolved organic matter. The cations in the M2E (water) sample followed the order $Na^+ > Ca^{2+} > K^+ > Mg^{2+} > NH_4^+$, with a lower ammonium value (0.5 mg/L) compared to a previous water analysis in a similar place before 2019, with a value of 40-30 mg/L N– NH_4^+. This indicates minimal stream input of dissolved ammonium. Relative to other cations, ammonium was not in the majority in either sample.

6. Discussion

It was confirmed that the persistent concentration of NH_4^+ in sediments affected by the stream current originated from 40 years of WWTP discharge. Both e-NH_4^+ (exchanged from clay) and d-NH_4^+ (from aqueous extracts) remained concentrated at intermediate depths (30–40 cm) relative to the high variability of near-surface samples and significantly decreased until virtually disappearing at locations deeper than 70 cm.

The NH_4^+ accumulation in sediments was consistent with the studied WWTP. The plant was designed for DOC treatment alone without nitrogen mitigation strategies for at least three decades until the process was updated to include an anoxic stage and a clarifier in 2019. The available historical data on nutrient analysis of the catchment and the discharge of the WWTP are scarce and were periodically collected by the internal maintenance service in response to discharge anomalies detected by hydrological basin authorities, which were followed by the consequential fines (UAM, infrastructure service communication, 2022, unpublished). Analyses performed before 2019 (2012–2017) at the catchment (1000-500 mg/L DOC) recorded 40-30 mg/L N–NH_4^+ and 5–10 mg/L N–NO_3^-, whereas the discharge contained 60-40 mg/L N–NH_4^+ and 5-2 mg/L N–NO_3^-. After 2019, data from 2020 to 2023, years with similar DOC and nitrogen values in the catchment, indicated that N–NH_4^+ was <1 mg/L and N–NO_3^- was 20-10 mg/L, which represents a significant improvement in the nitrogen decrease rate and less N–NH_4^+ discharge. This water quality change decreased ammonium inputs from 2020 and favoured slow natural nitrification. Stimulated nitrification is characteristic of this kind of headwater stream in which up to 100 % of the total streamflow used to be supplied by a WWTP, producing strong physical and chemical heterogeneity [49].

The erosion and sedimentation dynamics of materials transported by the stream flow determined the high variability observed in near-surface samples, as they exhibited the maximum and minimum measured ammonium values. The auger-sampled profiles could be classified into two main trends: (1) high NH_4^+ at the surface decreasing to a relatively constant value until 40–50 cm, where a progressive decrease with depth began until reaching minimum values at 70 cm and deeper locations (M2D sampling point); and (2) a low ammonium surface concentration leading to maximum values at 40–50 cm depth and decreasing until the 70 cm limit corresponding to the presence of nonpolluted sediment (M2C sampling point).

The first trend (1) is interpreted as the behaviour of a passive sediment bank with contaminated clay-rich sediment deposits, which retain the ammonium previously adsorbed by clay minerals. Relatively high pH values were measured (8.0–8.5) in high-ammonium (both soluble and exchangeable) surface samples. Near M2D, the M2B profile (previously sampled close to the stream) showed pH values between 7.0 and 5.3 (low ammonium concentration at the surface) and the evolution of ammonium to a maximum at 30–35 cm (pH 7.0); from this point, the pH increased to 8.0–8.3, and the ammonium content decreased with depth from 40 to 80 cm. This profile is more akin to the second trend (2), which is represented by the sampling point M2C, in which a critical decrease in pH to 4.0 was measured in surface samples to 15 cm depth and ammonium decreased until 60–70 cm depth. The pH increases when ammonium replaces other exchangeable cations in smectitic 2:1 clay minerals. Once NH_4^+ has saturated the interlayer region of the clay structure, the pH tends to decrease [50] due to the hydrolysis of the weak acid ($NH_4^+ \leftrightarrow NH_3 + H^+$) produced in cation exchange membranes, in which the pH decreases inside the membrane [51]. The drastic decrease in pH corresponds to sediments in an active erosion bank. Assuming that this sediment is continuously exposed to oxygen at the surface by periodic renewal due to sudden increases in water flow, both protons adsorbed in the exchanger and those produced in the nitrification process (overall equation without the NO_2^- intermediate step: $NH_4^+ + 2O_2 \leftrightarrow NO_3^- + H_2O + 2H^+$) contributed to this singular soil acidification. This acidification was not observed in the centre stream channel at the two sampling locations (M2E and M2A), where a hard, more clayey sediment is found. Inside the channel, there is less exposure to oxygen, and presumably, the sediment was progressively excavated by the stream (the location is characterized by older contamination). Then, surface exposure of the sediment and/or the clay content (as clay is less porous and permeable to gas and water) may have influenced the heterogeneity observed in the profiles. Small variations in clay (swelling smectite) content (i.e., 2–5 %) in consolidated sediments may induce several orders of magnitude decreases in hydraulic conductivity [52]. In fact, the influence of clay content can be confirmed by the observed limit at 70–80 cm depth, from which ammonium was virtually absent and which corresponded to a relatively enriched clayey band in transect M2D to M2C, which is discussed below.

The dynamics of contaminant dispersion in soil are complex, as they depend on several factors, including the attenuation of contamination, erosion, texture (clay content), and the nature of the sediments (Fig. 2).

Stream flow, which is variable, increases in situations where incoming water (storm water) exceeds the plant's treatment volume capacity. These fluctuations in river dynamics are highly likely to generate abrupt changes in erosion and sedimentation of materials in the channel [53]. This is particularly evident in the transect of three vertical samples (M2C, M2D and M2E). Point M2D had high

concentrations of total ammonium and the highest clay fraction concentration, with an average pH of 8.1 (Fig. 7). As previously discussed, this point represented a passive bank in which the ammonium could have accumulated years ago, when the treatment performance of the plant was not as efficient as could be desired. As seen from the comparison with point M2C, there was asymmetry in the margins. At this point, the highest ammonium concentration was isolated at a midpoint in the auger core, coinciding with the zone of highest clay concentration at that point. Just above this band, the pH decreased considerably to values close to 4.0. The anomalies in pH value and t-NH_4^+ concentration are due to erosion dynamics, although contributions from materials in this stream margin, that had not been polluted in the past, cannot be excluded, as erosion in the margin could disaggregate nonpolluted sandy materials that later deposited due to gravity.

Flushing is associated with the development of acidity in the soil, which is contrary to one of the highest exchangeable ammonium data points associated with acid pH. The presence of ammonium is significantly linked to its retention in the clay fraction [24], as shown by the predominance of exchangeable ammonium over soluble ammonium. Therefore, the washing and acidity detected in one of the margins could be attributed to a recent sediment deposit with extensive nitrification activity that has been reworked and is now free of ammonium contamination. These punctuated increases in water flow velocity may favour the washing of the sediment, and therefore, as mentioned above, decreases in ammonium and clay concentrations. At approximately 60 cm soil depth, there is a horizontal band of clay that probably serves as a containment system for ammonium since the contaminant decreases in concentration with depth until it practically disappears.

Corroborating the improvement in the WWTP system, the collected and analysed water samples showed a notable variation in the ammonium cation. In the water sample collected from the stream surface, M2E (water), the ammonium cation had a content of 0.5 mg/L. However, the sample that contained both stormwater and sediment runoff water, M2C (water), contained 7.4 mg/L. These values confirm that, at present, the discharge from the treatment plant has a very low ammonium concentration compared to that in past years, and other cations predominate because the conductivity remains high despite having slightly decreased.

The balance of nitrification and denitrification processes in the study area is not understood in detail, nor is it known whether volatilization processes even exist. It would be worth studying these dynamics and their relationship with the continuous changes in the energy and erosive capacity of the stream influenced by storms and WWTP discharge regimes in the future. Soil aquifer treatment (SAT) strategies are being studied to take advantage of natural attenuation to control nutrient discharges [54,55]. In future research, the studied location could be a good scenario to develop models for predicting the evolution of ammonium pollution.

Very small ammonium concentrations are observed at pH values higher than 8.5 because ammonium is transformed into ammonia gas [56]. The existence of a low-permeability clay barrier at depth (50–70 cm) could favour the development of hydromorphic and reducing conditions in the water-saturated sediment at depth. Then, presumably, oxidation processes do not occur easily due to the lack of dissolved oxygen due to pore saturation [57], which leads to the protection of the ammonium cation in the interlaminar region of smectites [58]. For this reason, pollution that was discharged years ago is still present in the sediment. Moreover, clays serve as an attenuation factor (retarding transport) [59]; consequently, these minerals can act as indicators that persist over time, providing a signature of the ammonium contamination formerly produced by the UAM WWTP.

The concept of a "geo-indicator" has commonly been used to refer to physical phenomena associated with geological risks, which are of interest for the extraction of geological resources [60]. More recently, increased interest has been shown in the study of chemical or physico-chemical phenomena associated with geo-indicators [61–64]] because they help to identify possible anthropogenic contaminants in the environment [65].

Monitoring natural areas affected by polluted discharges and their possible remediation dynamics, including natural attenuation processes, is important to assess actions towards zero pollution objectives. Such monitoring contributes to improving environmental quality standards and avoiding the impact of environmental deterioration on human health. The possibility of monitoring the evolution of pollution in stream sediments affected by the systematic discharge of effluent from a wastewater treatment plant with relatively high concentrations of nutrients has been studied. In this context, ammonium is likely the main source of nitrates, along with other nutrients, promoting eutrophication and contamination of aquifers [66,67]. Ammonium, due to its property of being adsorbed at cation exchange positions in 2:1 clay minerals [68], has been used as a geo-indicator [69] of the evolution of contamination. In the studied case, a geo-indicator is naturally present in the sediment and has attenuated the contamination caused by the effluent from the WWTP. Therefore, the smectite in the study area can be considered a passive geo-indicator.

The work carried out presents a series of limitations that must be mentioned. The significant variation in the distribution of ammonium in the shallowest sediments does not allow us to unequivocally differentiate the effects of erosion and transport dynamics, the rate of nitrification or the heterogeneity of the texture itself. It has been proposed to carry out detailed sampling in similar locations, in the near future, to check and clarify the origin of this heterogeneity and more accurately assess the role of natural attenuation in reducing the ammonium concentration in the discharge environment.

7. Conclusions

For approximately 50 years, a medium-sized WWTP has not operate efficiently. As a result, sediment contamination in the receiving stream remains to this day. Our study demonstrated that ammonium retention in clayey sediments is a reliable signature of a previously existing pollution source, although it is actually free of ammonium outflow. Ammonium transport downwards stopped beyond a band of clayey sediments (60–70 cm), whereas it remained concentrated at 30–40 cm depth, with a highly heterogeneous distribution in the near surface zones.

The statistical analysis showed that there was a direct relationship between higher total ammonium concentrations and clay content. Therefore, clay (smectite) in our study area served as a passive geo-indicator for ammonium contamination. The mechanical

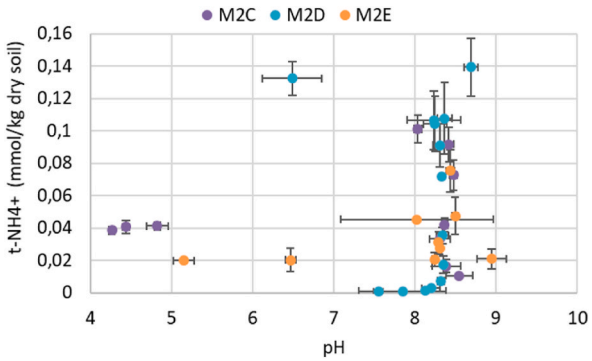

Fig. 7. Variations in pH and t-NH_4^+ concentration in the horizontal section.

dispersion of clay with adsorbed cation contamination and the roles of erosion and sedimentation processes, and nitrification, should be addressed by means of detailed sampling in the future.

Data availability statement

Data will be made available on request.

CRediT authorship contribution statement

María Tijero Martín: Data curation, Formal analysis, Investigation, Methodology, Validation, Visualization, Writing – original draft, Writing – review & editing. **Lucía Valdepeñas Polo:** Data curation, Formal analysis, Investigation, Methodology, Software, Validation, Visualization, Writing – original draft, Writing – review & editing. **Javier González Yélamos:** Conceptualization, Formal analysis, Investigation, Methodology, Supervision, Validation, Visualization, Writing – review & editing. **Jaime Cuevas Rodríguez:** Conceptualization, Formal analysis, Investigation, Methodology, Project administration, Resources, Software, Supervision, Validation, Visualization, Writing – original draft, Writing – review & editing.

Declaration of competing interest

The authors declare that they have no known competing financial interests or personal relationships that could have appeared to influence the work reported in this paper.

Appendix A. Supplementary data

Supplementary data to this article can be found online at https://doi.org/10.1016/j.heliyon.2023.e21860.

References

[1] Who, Unicef, World Bank, State of the World's Drinking Water: an Urgent Call to Action to Accelerate Progress on Ensuring Safe Drinking Water for All, World Health Organization, Geneva, 2022, 2022. Licence: CC BY-NC-SA 3.0 IGO. 114pp.
[2] EU Commission, EU Action Plan: 'Towards Zero Pollution for Air, Water and Soil'. Brussels, 12.5.2021, 2021. COM (2021) 400 final. COMMUNICATION FROM THE COMMISSION TO THE EUROPEAN PARLIAMENT, THE COUNCIL, THE EUROPEAN ECONOMIC AND SOCIAL COMMITTEE AND THE COMMITTEE OF THE REGIONS EMPTY. Pathway to a Healthy Planet for All. 21pp.
[3] C. Vörösmarty, P. McIntyre, M. Gessner Dudgeon, A. Prusevich, P. Green, S. Glidden, S.E. Bunn, C.A. Sullivan, C. Reidy Liermann, P.M. Davies, Global threats to human water security and river biodiversity, Nature 467 (2010) 555–561, https://doi.org/10.1038/nature09440.
[4]] M.T.H. van Vliet, J.J.G. Zwolsman, Impact of summer droughts on the water quality of the Meuse river, J. Hydrol. 353 (2008) 1–17, https://doi.org/10.1016/j.jhydrol.2008.01.001.
[5] M.N. Khan, M. Mobin, Z.K. Abbas, S.A. Alamri, Fertilizers and their contaminants in soils, surface and groundwater, in: Dominick A. DellaSala, Michael I. Goldstein (Eds.), The Encyclopedia of the Anthropocene, vol. 5, 2018, pp. 225–240, https://doi.org/10.1016/B978-0-12-809665-9.09888-8, 9780128135761.
[6] P. Shi, Y. Zhang, J. Song, P. Li, Y. Wang, Xiaoming Zhang, Z. Li, Z. Bi, Xin Zhang, Y. Qin, T. Zhu, Response of nitrogen pollution in surface water to land use and social-economic factors in the Weihe River watershed, northwest China, Sustain. Cities Soc. 50 (2019), 101658, https://doi.org/10.1016/j.scs.2019.101658.
[7] L. Sun, X. Liang, M. Jin, B. Ma, X. Zhang, C. Song, Ammonium and Nitrate Sources and Transformation Mechanism in the Quaternary Sediments of Jianghan Plain, China, Science of The Total Environment, 774, 2021, 145131, https://doi.org/10.1016/j.scitotenv.2021.145131.
[8] J.A. Camargo, A. Alonso, Contaminación por nitrógeno inorgánico en los ecosistemas acuáticos: problemas medioambientales, criterios de calidad del agua, e implicaciones del cambio climático, Ecosistemas 16 (2) (2007) 1–13. ISSN: 1132-6344.
[9] Y. Zhang, Z. Chen, G. Huang, M. Yang, Origins of groundwater nitrate in a typical alluvial-pluvial plain of North China plain: new insights from groundwater age-dating and isotopic fingerprinting, Environ. Pollut. 316 (2023), 120592, https://doi.org/10.1016/j.envpol.2022.120592. ISSN 0269-7491.
[10] G.L. Cárdenas Calvachi, I.A. Sánchez Ortiz, Nitrogen in Wastewater: Origins, Effects and Removal Mechanisms to Preserve the Environment and Public Health vol. 15, Universidad y Salud, 2013, pp. 72–88. ISSN 0124-7107.

[11] C. Díez-Mayáns, R. Bienes, Evolución de la contaminación por nitratos, nitritos y amonio en los ríos Henares, Tajuña, Jarama y Tajo de la Comunidad de Madrid. I Simposio nacional sobre el control de la erosión y degradación del suelo, 2003, pp. 143–148.

[12] Y. Liu, H.H. Ngo, W. Guo, L. Peng, D. Wang, B. Ni, The roles of free ammonia (FA) in biological wastewater treatment processes: a review, Environ. Int. 123 (2019) 10–19, https://doi.org/10.1016/j.envint.2018.11.039. ISSN 0160-4120.

[13] P.F. Molina, P.J.M. Fernández, P.I. Miralles, A.C. Sánchez, J.L.A. Soto, M.G.L. Sánchez, E. Mercader, Estudio técnico de caracterización del perfil de nutrientes de la rambla del Albujón y su relación con la, EDAR Torre Pacheco, 2022, p. 27.

[14] D. Dominguez, W. Gujer, Evolution of a wastewater treatment plant challenges traditional design concepts, Water Res. 40 (2006) 1389–1396, https://doi.org/10.1016/j.watres.2006.01.034.

[15] S.R. Buss, A.W. Herbert, P. Morgan, et al., A review of ammonium attenuation in soil and groundwater, Q. J. Eng. Geol. Hydrogeol. (2004) 347–359, https://doi.org/10.1144/1470-9236/04-005.

[16] Y. Li, H. Li, S. Xiao, S. Xu, X. Xu, S. Wang, Fate of nitrogen in subsurface infiltration system for secondary effluent treatment, Water Sci. Eng. 10 (2017) 217–224, https://doi.org/10.1016/j.wse.2017.10.002. ISSN 1674-2370.

[17] H.L. Bohn, B.L. McNeal, G.A. O'Connor, Soil Chemistry, 3rd. ed., John Wiley & Sons, New York, 2001, p. 307.

[18] S. Eturki, F. Ayari, N. Jedidi, H. Ben Dhia, Use of clay mineral to reduce ammonium from wastewater. Effect of various parameters, Surf. Eng. Appl. Electrochem. 48 (2012) 276–283, https://doi.org/10.3103/S1068375512030064.

[19] M. Rautureau, C. Gomes, N. Liewig, M. Katouzian-Safadi, Clays and Health Properties and Therapeutic Uses, Springer International Publishing AG, Cham, Switzerland, 2017, p. 217, https://doi.org/10.1007/978-3-319-42884-0.

[20] A. Alshameri, H. He, J. Zhu, Y. Xi, R. Zhu, L. Ma, Q. Tao, Adsorption of ammonium by different natural clay minerals: characterization, kinetics and adsorption isotherms, Appl. Clay Sci. 159 (2018) 83–93, https://doi.org/10.1016/j.clay.2017.11.007. ISSN 0169-1317.

[21] R. Nieder, D.K. Benbi, D.W. Scherer, Ammonium fixation and defixation in soils: a review, Biol. Fertil. Soils 47 (2011) 1–14, https://doi.org/10.1007/s00374-010-0506-4.

[22] X. Wang, X. Wang, W. Zhao, R. Yu, J. Wu, Y. Kou, Q. Liu, W. Zhao, Differential bacterial ammonia oxidation patterns in soil particles from two contrasting forests: the importance of interfacial interactions, Geoderma 429 (2023), 116255, https://doi.org/10.1016/j.geoderma.2022.116255. ISSN 0016-7061.

[23] M.L. Whittaker, N.L. Lammers, S. Carrero, B. Gilbert, J.F. Banfield, Ion exchange selectivity in clay is controlled by nanoscale chemical-mechanical coupling, Proceedings of the National Academy of Sciences. PNAS 116 (2019) 22052–22057, https://doi.org/10.1073/pnas.1908086116.

[24] S.R. Buss, A.W. Herbert, P. Morgan, S.F. Thornton, Review of ammonium attenuation in soil and groundwater. National groundwater and contaminated land centre, Technical Report, https://doi.org/10.13140/RG.2.1.2206.7604, 2003.

[25] M. Regadío, A.I. Ruiz, M. Rodríguez-Rastrero, J. Cuevas, Containment and attenuation layers: an affordable strategy that preserves soil and water from landfill contamination, Waste Manag. 46 (2015) 408–419, https://doi.org/10.1016/j.wasman.2015.08.014. ISSN 0956-053X.

[26] S. Hulth, R.C. Aller, F. Gilbert, Coupled anoxic nitrification/manganese reduction in marine sediments, Geochem. Cosmochim. Acta 63 (1) (1999) 49–66, https://doi.org/10.1016/S0016-7037(98)00285-3.

[27] I. Schmidt, O. Sliekers, M. Schmid, I. Cirpus, M. Strous, E. Bock, J. Kuenen, G, M. Jetten, Aerobic and anaerobic ammonia oxidizing bacteria - competitors or natural partners? FEMS (Fed. Eur. Microbiol. Soc.) Microbiol. Ecol. 39 (2002) 175–181, https://doi.org/10.1111/j.1574-6941.2002.tb00920.x.

[28] B. Thamdrup, T. Dalsgaard, Production of N2 through anaerobic ammonium oxidation coupled to nitrate reduction in marine sediments, Appl. Environ. Microbiol. 68 (2002) 1312–1318, https://doi.org/10.1128/AEM.68.3.1312-1318.2002.

[29] Y. Umezawa, T. Hosono, S.I. Onodera, F. Siringan, S. Buapeng, R. Delinom, C. Yoshimizu, I. Tayasu, T. Nagata, M. Taniguchi, Sources of nitrate and ammonium contamination in groundwater under developing Asian megacities, Sci. Total Environ. 404 (2008) 361–376, https://doi.org/10.1016/j.scitotenv.2008.04.021.

[30] P.L. Bjerg, N. Tuxen, L.A. Reitzel, H.-J. Albrechtsen, P. Kjeldsen, Natural attenuation processes in landfill leachate plumes at three Danish sites, Groundwater 49 (2011) 688–705, https://doi.org/10.1111/j.1745-6584.2009.00613.x.

[31] T.H. Christensen, P. Kjeldsen, P.L. Bjerg, D.L. Jensen, J.B. Christensen, A. Baun, H.-J. Albrechtsen, G. Heron, Biogeochemistry of landfill leachate plumes, Appl. Geochem. 16 (7–8) (2001) 659–718, https://doi.org/10.1016/S0883-2927(00)00082-2. ISSN 0883-2927.

[32] U. Maier, H. Rügner, P. Grathwohl, Gradients controlling natural attenuation of ammonium, Appl. Geochem. 22 (12) (2007) 2606–2617, https://doi.org/10.1016/j.apgeochem.2007.06.009. ISSN 0883-2927.

[33] Spain. Ley 16/1995, de 4 de mayo, Forestal y de Protección de la Naturaleza, Boletín Oficial del Estado, 4 de mayo de 1995, nº190, pp. 24949-24972. [Accessed 23 April 2023]. Available at: https://www.boe.es/buscar/doc.php?id=BOE-A-1995-19108.

[34] Confederación Hidrográfica del Tajo, Plan Hidrológico de la parte española de la Demarcación Hidrográfica del Tajo (2015-2021), 2015, p. 130 [Accessed 23 April 2023]. Available at: https://transparencia.gob.es/servicios-buscador/contenido/planesprogramas.htm?id=PLANESPROGRAMAS_142&lang=gl.

[35] Comunidad de Madrid, Masas de agua subterránea de la Comunidad de Madrid, 2022, p. 2 [Accessed 23 April 2023]. Available at: https://www.comunidad.madrid/sites/default/files/doc/medio-ambiente/masas_de_agua_subterranea_ver3.pdf.

[36] Instituto Geológico y Minero de España, Mapa Geológico Nacional Segunda Serie, 2000. Hoja 534, escala 1:50000. [Accessed 23 April 2023], http://info.igme.es/cartografiadigital/geologica/Magna50Hoja.aspx?language=es&id=534.

[37] Ayuntamiento de Alcobendas, Revisión y adaptación del plan general de Alcobendas, 2005. Estudio de caracterización de suelo. [Accessed 23 April 2023]. Available at: https://www.alcobendas.org/sites/default/files/2021-04/Estudio%20caracterizaci%C3%B3n%20del%20suelo.pdf.

[38] Ministerio de Hacienda y Función Pública, Gobierno de España, Expediente O-11/18, 2018. Available at: https://contrataciondelestado.es/wps/portal/!ut/p/b0/Dcq9CoAgEADgB2q4NiNoiHC3JX-WONLi6LQMsdev8YMPHBhwCSsdWOhKyL-tDFmSmfvQ0HmsDJtVHD7A2hw4MjLymB3lRuh45O7ycxLq6Vgq95hgDvG8QNnZhMl/. (Accessed 12 May 2022).

[39] Spain Real Decreto 509/1996, de 15 de marzo, de desarrollo del Real Decreto-ley 11/1995, de 28 de diciembre, por el que se establecen las normas aplicables al tratamiento de las aguas residuales urbanas. Boletín Oficial del Estado, 15 de marzo de 1996, nº77, pp. 12038-12041. [Accessed 23 April 2023]. Available at: https://www.boe.es/eli/es/rd/1996/03/15/509.

[40] S. Martínez-Campos, M. González-Pleiter, F. Fernández-Piñas, R. Rosal, F. Leganés, Early and differential bacterial colonization on microplastics deployed into the effluents of wastewater treatment plants, Sci. Total Environ. 757 (2021), 143832, https://doi.org/10.1016/j.scitotenv.2020.143832.

[41] D.E. Kissel, M.L. Cabrera, Ammonia, in: D. Hillel (Ed.), Reference Module in Earth Systems and Environmental Sciences: Encyclopedia of Soils in the Environment, Elsevier Ltd., Amsterdam, 2005, pp. 56–64.

[42] J. Porta, Methodologies for the analysis and characterization of gypsum in soils: a review, Geoderma 87 (1–2) (1998) 31–46, https://doi.org/10.1016/S0016-7061(98)00067-6.

[43] J. Choosang, A. Numnuam, P. Thavarungkul, P. Kanatharana, T. Radu, S. Ullah, A. Radu, Simultaneous detection of ammonium and nitrate in environmental samples using on ion-selective electrode and comparison with portable colorimetric assays, Sensors 18 (10) (2018) 3–555, https://doi.org/10.3390/s18103555.

[44] G.W. Gee, D. Or, Particle-size analysis, in: Jacob H. Dane, G. Clarke Topp, Coeditors (Eds.), Methods of Soil Analysis, Part 4, Physical Methods", Soil Science Society of America Book Series, 5, Soil Science Society of America, Inc. Madison, Wisconsin, USA, 2002, pp. 255–294, 978-0-891-18893-3.

[45] M.A. Correa, S.A. Franco, L.M. Gómez, D. Aguiar, H.A. Colorado, Characterization methods of ions and metals in particulate matter pollutants on PM2. 5 and PM10 samples from several emission sources, Sustainability 15 (5) (2023) 4402, https://doi.org/10.3390/su15054402.

[46] Thermo Fisher Scientific, Standard Ammonia Ion Selective Electrode User Manual. [Equipment], 2009, p. 47 [Accessed 23 April 2023], https://assets.fishersci.com/TFS-Assets/LSG/manuals/D01250~.pdf.

[47] P. Seruga, M. Krzywonos, J. Pyżanowska, A. Urbanowska, H. Pawlak-Kruczek, Ł. Niedźwiecki, Removal of ammonia from the municipal waste treatment effluents using natural minerals, Molecules 24 (2019) 3633, https://doi.org/10.3390/molecules24203633.

[48] T. Liu, L. Mu, X. Li, Y. Li, Z. Liu, X. Jiang, C. Feng, L. Zheng, Characteristics and Source Apportionment of Water-Soluble Inorganic Ions in Atmospheric Particles in Lvliang, China, Environmental Geochemistry and Health, 2023, pp. 1–15, https://doi.org/10.1007/s10653-023-01484-0.

[49] S.N. Merbt, J.-C. Auguet, A. Blesa, E. Martí, E.O. Casamayor, Wastewater treatment plant effluents change abundance and composition of ammonia-oxidizing microorganisms in mediterranean urban stream biofilms, Microb. Ecol. 69 (2015) 66–74, https://doi.org/10.1007/s00248-014-0464-8.

[50] M. Gautier, F. Muller, L. Le Forestier, J.-M. Beny, R. Guegan, NH4-smectite: characterization, hydration properties and hydromechanical behavior, Appl. Clay Sci. 49 (2010) 247–254, https://doi.org/10.1016/j.clay.2010.05.013. ISSN 0169-1317.
[51] O. Kozaderova, O. Kozaderov, S. Niftaliev, Electromass transfer in the system "cation exchange membrane—ammonium nitrate solution", Membranes 12 (2022) 1144, https://doi.org/10.3390/membranes12111144.
[52] A.I. Ruiz, R. Fernández, N. Sánchez, M. Rodríguez Rastrero, M. Regadío, I. de Soto, J. Cuevas, Improvement of the attenuation functions of a clayey sandstone for landfill leachate containment by the addition of bentonite, Sci. Total Environ. 419 (2012) 81–89, https://doi.org/10.1016/j.scitotenv.2011.11.054. ISSN 0048-9697.
[53] V. Pardo, Estudio de la sedimentación y erosión producida en la red de saneamiento de la ciudad de Murcia, Universidad Politécnica de Cartagena, Cartagena, 2017, p. 159.
[54] A. Abu, R. Carrey, C. Valhondo, C. Domènech, A. Soler, L. Martínez-Landa, S. Diaz-Cruz, J. Carrera, N. Otero, Pathways and efficiency of nitrogen attenuation in wastewater effluent through soil aquifer treatment, J. Environ. Manag. 321 (2022), 115927, https://doi.org/10.1016/j.jenvman.2022.115927. ISSN 0301-4797.
[55] J. Sallwey, A. Jurado, F. Barquero, J. Fahl, Enhanced removal of contaminants of emerging concern through hydraulic adjustments in soil aquifer treatment, Water 12 (2020) 2627, https://doi.org/10.3390/w12092627.
[56] Q. Li, Y. Xu, C. Liang, L. Peng, Y. Zhou, Nitrogen Removal by Algal-Bacterial Consortium during Mainstream Wastewater Treatment: Transformation Mechanisms and Potential N2O Mitigation, Water Research, 2023, 119890, https://doi.org/10.1016/j.watres.2023.119890. ISSN 0043-1354.
[57] R. Yupiter, S. Arnon, E. Yeshno, I. Visoly-Fisher, O. Dahan, Real-time detection of ammonium in soil pore water, npj Clean Water 6 (1) (2023) 25, https://doi.org/10.1038/s41545-023-00243-z.
[58] T. Li, Z. Wang, C. Wang, J. Huang, Y. Feng, W. Shen, M. Zhou, L. Yang, Ammonia volatilization mitigation in crop farming: a review of fertilizer amendment technologies and mechanisms, Chemosphere (2022), 134944, https://doi.org/10.1016/j.chemosphere.2022.134944. ISSN 0045-6535.
[59] T.T. Hoai, T. Mukunoki, M.T. Nhuan, N.T.H. Ha, Temperature and concentration dependence of ammonium migration in bentonite-clay mixtures: a case study in Hanoi, Vietnam, Soils Found. 63 (1) (2023), 101251, https://doi.org/10.1016/j.sandf.2022.101251.
[60] A.R. Berger, Environmental change, geoindicators, and the autonomy of nature, GSA Today (Geol. Soc. Am.) 8 (1) (1998) 3–8.
[61] W.F. Giggenbach, Geothermal solute equilibria. derivation of Na-K-Mg-Ca geo-indicators, Geochem. Cosmochim. Acta 52 (12) (1988) 2749–2765, https://doi.org/10.1016/0016-7037(88)90143-3. ISSN 0016-7037.
[62] G. Birch, Use of sedimentary-metal indicators in assessment of estuarine system health, in: J. Shroder, A.D. Switzer, D.M. Kennedy (Eds.), Treatise on Geomorphology, Academic Press, San Diego, CA, USA, 2013, pp. 282–291.
[63] B.E. García-Sánchez, G.M. Vara-Castro, T. Kretzschmar, J.I. Sánchez-Avila, Organic compounds in surface and groundwaters in the surrounding of a Mexican geothermal reservoir; case study Los Humeros, Puebla, Appl. Geochem. 147 (2022), 105442, https://doi.org/10.1016/j.apgeochem.2022.105442. ISSN 0883-2927.
[64] M.A. Benamar, H. Azzaz, A.K. Khaldi, Chemical Geothermometers and Mixing Models to Understand the Thermal Aptitudes in the Management of Bouhanifia and Saida Geothermal Resources, Northwest of Algeria, Groundwater for Sustainable Development, 20, 2023, 100863, https://doi.org/10.1016/j.gsd.2022.100863. ISSN 2352-801X.
[65] A.R. Berger, R.A. Hodge, Natural change in the environment: a challenge to the pressure-state-response concept, Soc. Indicat. Res. 44 (2) (1998) 255–265, https://doi.org/10.1023/A:1006888532080.
[66] S. Jellali, E. Diamantopoulos, H. Kallali, S. Bennaceur, M. Anane, N. Jedidi, Dynamic sorption of ammonium by sandy soil in fixed bed columns: evaluation of equilibrium and non-equilibrium transport processes, J. Environ. Manag. 91 (4) (2010) 897–905, https://doi.org/10.1016/j.jenvman.2009.11.006.
[67] S. Shen, T. Ma, Y. Du, Z. Han, J. Zhang, W. Liu, K. Luo, Contrastive mechanisms of groundwater ammonium enrichment in different hydrogeologic settings, Sci. Total Environ. 875 (2023), 162542, https://doi.org/10.1016/j.scitotenv.2023.162542.
[68] J. Cuevas, D.E. González-Santamaría, C. García-Delgado, A. Ruiz, A. Garralón, A.I. Ruiz, R. Fernández, E. Eymar, R. Jiménez-Ballesta, Impact of a tire fire accident on soil pollution and the use of clay minerals as natural geo-indicators, Environ. Geochem. Health 42 (2020) 2147–2161, https://doi.org/10.1007/s10653-019-00485-2.
[69] A.R. Berger, Assessing rapid environmental change using geoindicators, Environ. Geol. 32 (1) (1997) 36–44, https://doi.org/10.1007/s002540050191.